# Hypervalent Compounds as Ligands: I_3-Anion Adducts with Transition Metal Pentacarbonyls

Andrey Yu. Rogachev and Roald Hoffmann*

Baker Laboratory, Department of Chemistry and Chemical Biology, Cornell University, Ithaca, New York 14853, United States

ⓢ *Supporting Information*

ABSTRACT: Just a couple of transition metal complexes of the familiar triiodide anion are known. To investigate the bonding in these, as well as isomeric possibilities, we examined theoretically adducts of I_3^- with model organometallic fragments, $[Cr(CO)_5]$ and $[Mn(CO)_5]^+$. Bonding energy computations were augmented by a Natural Bond Orbital (NBO) perturbation theory analysis and Energy Decomposition Analysis (EDA). The bonding between I_3^- and the organometallic fragment is substantial, especially for the electrostatically driven anion−cation case. "End-on" coordination is favored by 5−13 kcal/mol over "side-on" (to the central I of I_3^-), with a ~10 kcal/mol barrier for isomerization. A developing asymmetry in the I−I bonding of "end-on" coordinated I_3^- led us to consider in some detail the obvious fragmentation to a coordinated I^- and free I_2. While the signs of incipient fragmentation in that direction are there, these is a definite advantage to maintaining some I^- to I_2 bonding in triiodide complexes.
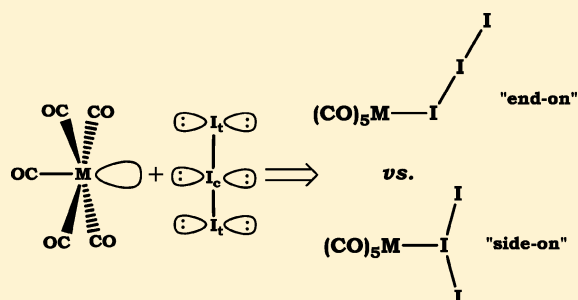
■ INTRODUCTION

The chemistry of iodine and compounds based on iodine is amazingly rich and diverse. The atom itself differs significantly from other halogens only in size and softness, not, for instance, in electron affinity. Large in atomic size, possessing that high electron affinity and a low ionization potential, the iodine atom can easily form stable polycoordinate and multivalent compounds.

The diatomic iodine molecule, only weakly bound with respect to atomization, also has a diverse chemistry. In the electronic structure of simple diatomic I_2 (and its color), one sees immediately its characteristic acceptor and donor features: a relatively low-lying LUMO (lowest unoccupied molecular orbital) and the relatively high-lying HOMO (highest occupied molecular orbital).

These features of I, I^-, and I_2 make them almost ideal building blocks for reaction not only with other molecules, but also with each other. Indeed, the structural chemistry of polyiodides is fascinating. Polyiodides abound, from very simple discrete units to one-dimensional chains and on to more complicated two- and three-dimensional networks.[1] The simplest representative of I^- and I_2 chemistry is the triiodide ion I_3^-, **1**. The symmetrical ion occurs with many counterions. It is a prototypical electron-rich three-center bonded system,[2] quite analogous to the related XeF_2, and finding a counterpart in other trihalide ions, X_3^-, X = Br, Cl, F.

The symmetrical triiodide ion has an equilibrium distance of 2.96 Å, and a (gas phase) bonding energy of −38 kcal/mol relative to I^- and I_2 (2.69 Å). As an early insight by Henry Bent showed,[3] the crystal structures of triiodide complexes trace out a beautiful hyperbolic continuum of one bond strengthened
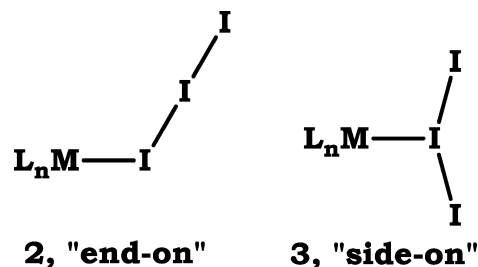
(shortened), the other weakened (lengthened) in the hundreds of complexes known. This is shown in a classical Bürgi−Dunitz diagram[4] (Figure 1), an updated version of one found in the excellent review of Svensson and Kloo.[1]

Given the diverse chemistry of I, I^-, and I_2, among themselves, one would expect many metal complexes of these molecular units. This expectation is not met. There are a number of organometallic iodides. But we have found only four I_2 complexes; remarkably, in three of these I_2 acts as an acceptor, and in one, just one, as a classical donor. The unusual bonding in these is discussed in recent paper by us.[5]

In this contribution, part of an exploration of hypervalent molecules as ligands, we concentrate on the simplest of the polyiodides, I_3^-, as a ligand. Throughout this Article, we will refer to extrema of what may be a continuum of bonding of this triatomic entity as "end-on" (**2**) or "side-on" (**3**) coordination to a metal center.

The chemistry of polyiodides as ligands for metal fragments, both inorganic and organometallic, is actually reasonably
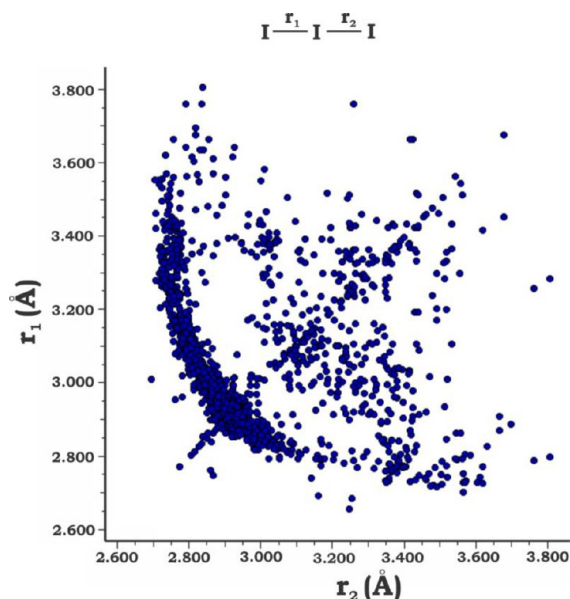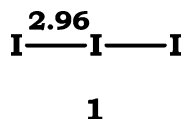
Figure 1. Statistical overview of the triiodide ion structure.

1

developed. However, most of the relevant structural data in the Cambridge Structural Database (CSD)[6] corresponds to

interaction between polyiodide chains (infinite or oligomeric fragments) and metal complexes. One can find in such chains more or less defined building blocks, derived from I^-, I_2, I_3^- and their associations. The number of I_2 building blocks determines the length of the polyiodide chain.[1] The degree of iodine association makes it difficult to describe the M–I bonding, or even just the coordination geometry, as "end-on" and "side-on".

There are just a couple of well-defined examples of discrete molecular complexes of transition metal fragments with I_3^-. One comes from the work of Wieghardt et al.,[7] who isolated an adduct of I_3^- with tetracoordinated Ni(II) in the complex shown in Figure 2a. Clearly, coordination here is of the "end-on" type. Also "end-on" bound is I_3^- in the remarkable Pt(II) complex with a pincer-type organic ligand, synthesized by the group of G. van Koten (Figure 2b).[8] The van Koten compound is unique, due to the presence in one molecular transition metal complex of two different coordinated iodine-based fragments.

This meager structural data, as well as a general interest in hypervalent molecules as ligands, prompted us to a comprehensive theoretical investigation of the bonding in triiodide complexes. Is this the only way that I_3^- can coordinate "end-on"? Or can one stabilize "side-on" bonded I_3^-? Will coordinated I_3^- fall apart to I^- and neutral I_2?

As prototypic transition metal bonding partners for iodine-based ligands, two isolobal fragments will be considered: (i) neutral $Cr(CO)_5$ and (ii) cationic $Mn(CO)_5^+$. This will give us a chance to judge the effect of electrostatics on bond formation. A detailed study of energetics of the adducts of these fragments with I_3^-, I^-, and I_2 is complemented by in-depth investigation of their electronic structures by different theoretical approaches.
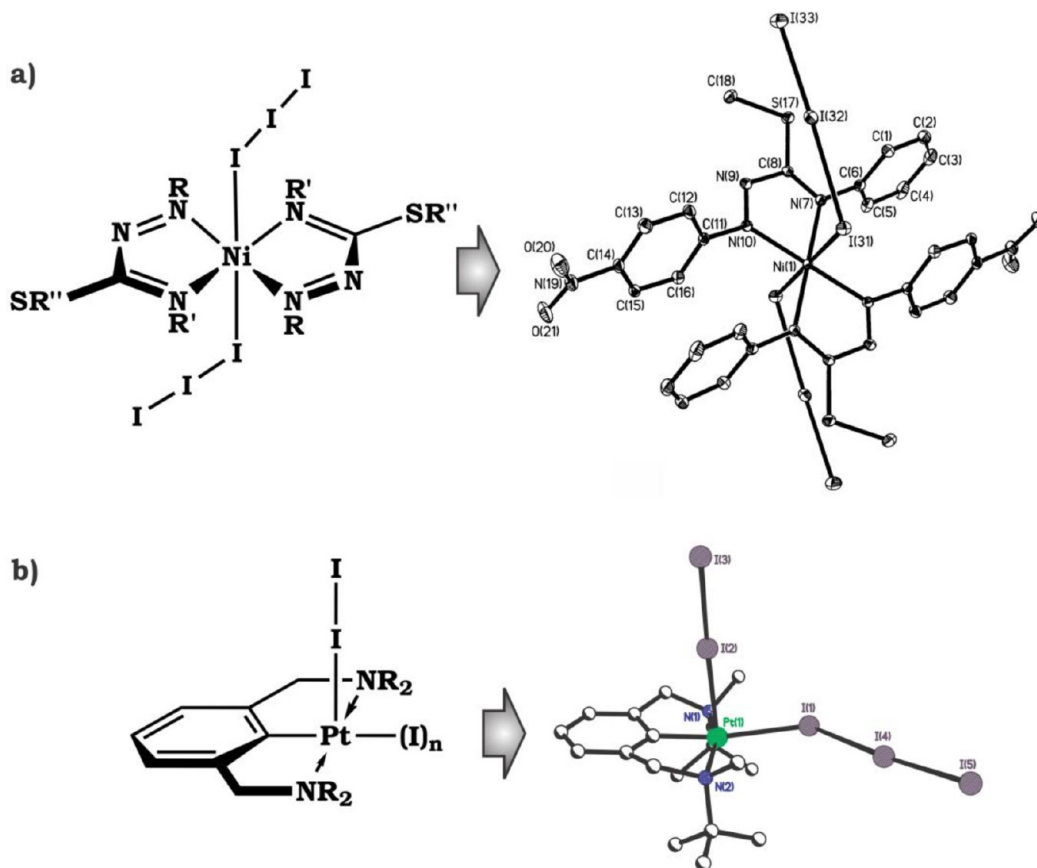

Figure 2. Adducts of I_3^- investigated by (a) Wieghardt et al.[7] and (b) van Koten et al.[8] Schematic ChemDraw representations and crystal structures.

The details of the computations are reported in the Appendix to this Article.

RESULTS AND DISCUSSION

Parent Fragments: M(CO)$_5$ and I$_3^-$. Before discussing the adducts of I$_3^-$ with selected metal pentacarbonyls, it is instructive to look at the fragments, M(CO)$_5$ and I$_3^-$.

The electronic structure of the d^6 M(CO)$_5$ fragment (for neutral species M = Cr, Mo, W, for monocationic ones M = Mn, Tc, Re, etc.) is well-known.[9] The most important feature of these Lewis acids is the presence of a low-lying empty acceptor orbital of a_1 symmetry, the outcome of hybridization of $(n + 1)$s and $(n + 1)$p with the nd orbital. The calculated shape of this orbital (note the π-bonding admixture with the carbonyls) as well as a schematic orbital diagram of the fragment, as it is derived from an ideal octahedron by removing a CO, is depicted in Figure 3. The shape of this orbital will be
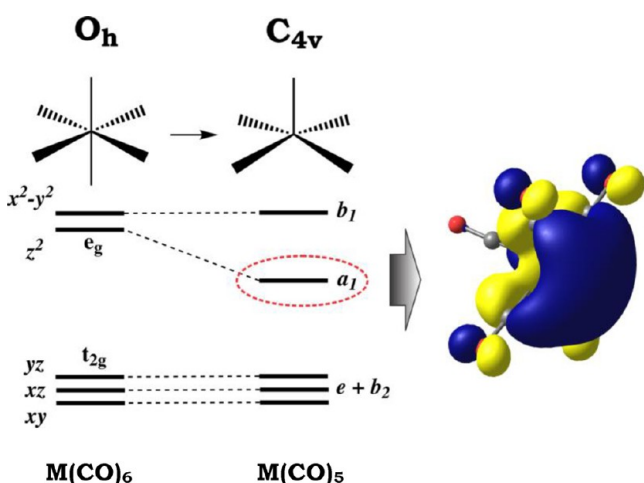

Figure 3. Orbital diagrams for M(CO)$_6$ (O_h) and M(CO)$_5$ (C_{4v}) (left). The latter is the consequence of removal of one carbonyl from M(CO)$_6$. At right is the resulting shape of the acceptor orbital (LUMO, a_1) in a Cr(CO)$_5$ fragment.

somewhat different in an NBO analysis, as we will see. The use of d^6 M(CO)$_5$ fragments, good Lewis acids, to bond lone pairs is common; for a selection, see recent work.[10]

I$_3^-$ is the archetypical octet-expanded triatomic species. The accepted bonding picture in this ubiquitous ion[1] is that of 4-electron−3-center (4e−3c) type bonding (Figure 4), residing
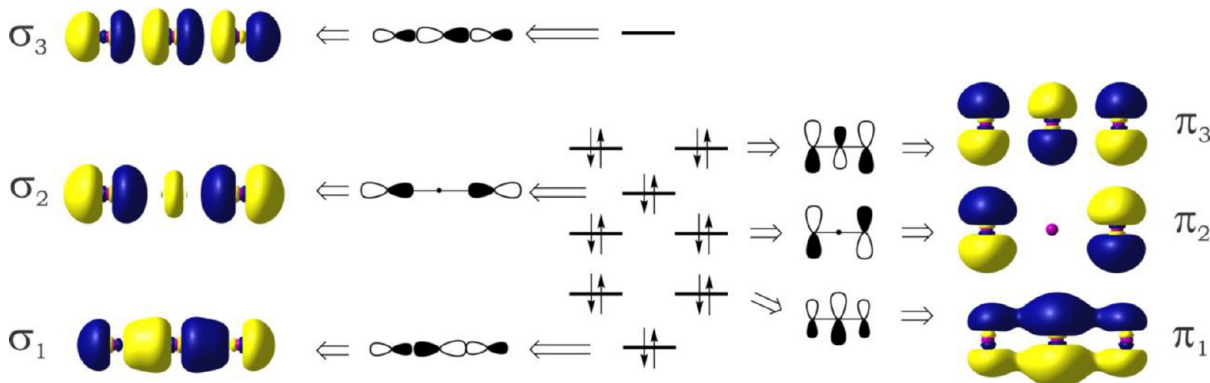
in the σ-system of the ion (for a detailed analysis of the bonding in I$_3^-$ and related compounds, see our earlier work[11] as well as the recent study of Wolters and Bickelhaupt[12]). A complete description of the reactivity of I$_3^-$ must include the π-type lone pairs (π_1, π_2, π_3 at right in Figure 4, all occupied) and the slight antibonding in the top filled σ orbitals, σ_2. The HOMO of the molecule is actually the upper-most lone pair π-combination (π_3), as shown in Figure 4. This degenerate orbital is antibonding between the iodine atoms. In our calculations it lies ~0.5 eV above the σ_2-orbital.

Where might a Lewis acid interact with I$_3^-$? The HOMO π_3 is slightly more localized on the central iodine. Not far below it in energy is σ_2, primarily localized on the end I's. This orbital actually determines the charge distribution in the triiodide anion, which calculated (NBO charges) to be −0.07 and −0.46 for the central iodine (I$_c$) and the terminal iodines (I$_t$), respectively. The nature of the HOMO argues for interaction at I$_c$ with a Lewis acid; the electrostatics argue for coordination at I$_t$. Another point of interest in the electronic structure of the I$_3^-$ molecular fragment is the presence of the relatively low-lying ($\Delta E_{LUMO-HOMO} = 3.70$ eV) and energetically well-isolated ($\Delta E_{(LUMO-1)-LUMO} = 7.59$ eV) σ_3 LUMO. This molecular orbital is the most antibonding combination of σ-type p-orbitals on iodines, the top (unoccupied) orbital in the classical 3c−4e bonding scheme. So, I$_3^-$ can also act as a potential acceptor, through its low-lying σ_3 LUMO. Though a significant population of σ_3 will break the molecule apart, I$_3^{3-}$ is like Xe$_3$.

"Side-On" Adducts of I$_3^-$. Indeed, calculations revealed that compounds of formula [Cr(CO)$_5$·I$_3$]$^-$-"side-on" and [Mn(CO)$_5$·I$_3$]-"side-on", the metal bonded to I$_c$, both correspond to minima on their potential energy surfaces (Figure 5a). We will explore the energetics of the bonding and
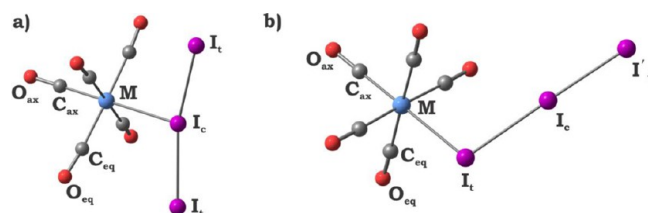
Figure 5. Equilibrium geometry configurations for: (a) [M(CO)$_5$·I$_3$]$^{n-}$-"side-on" and (b) [M(CO)$_5$·I$_3$]$^{n-}$-"end-on" ($n = 1$ for M = Cr and $n = 0$ for M = Mn) along with labeling scheme.

the relative energies of the two minima below; here we just analyze the "side-on" isomer. Selected geometrical parameters

Figure 4. Schematic depiction of the MO diagram for I$_3$-anion.

Table 1. Selected Geometrical Parameters for $[M(CO)_5 \cdot I_3]^{n-}$-"Side-On", $[M(CO)_5 \cdot I_3]^{n-}$-"Side-On" (n = 1 for M = Cr and n = 0 for M = Mn), and I_3^- (Bond Lengths in Å, Angles in Degrees)

	Cr			Mn			
	$[Cr(CO)_5 \cdot I_3]^-$			$[Mn(CO)_5 \cdot I_3]$			
param	"side-on"	"end-on"	$[Cr(CO)_5]$	"side-on"	"end-on"	$[Mn(CO)_5]^+$	I_3^-
$M-I^a$	2.80	2.78		2.73	2.70		
I_c-I_t	2.97	3.06		2.94	3.31		2.96
$I_c-I'_t$		2.86			2.74		2.96
$M-C_{eq}$	1.89	1.82	1.90	1.87	1.80	1.89	
$M-C_{ax}$	1.82	1.89	1.83	1.81	1.86	1.82	
$\angle I_t-I_c-I'_t$	167	179		170	179		180
$\angle C_{ax}-M-I^a$	180	180		180	180		
$\angle M-I^a-I$	97	108		95	104		
$\angle C_{eq}-M-I^*-I$	43	45		45	45		

^{a}The iodine atom connected to the metal center is I_c for "side-on" and I_t for "end-on" adducts, respectively.

are collected in Table 1. The use of extended basis sets (TZVPP instead of TZVP) or those containing an effective core potential (def-TZVPP + ECP) has no significant effect on the computed geometrical parameters of the systems under investigation. The same is true for the use of the "chain-of-spheres" (RIJCOSX) approximation. Thus, hereafter all analysis will be performed at the RIJCOSX-PBE0/SARC-TZVP/ZORA level of theory, a good compromise between accuracy and computational costs. All data sets obtained by using the other theoretical approaches mentioned above are presented in the Supporting Information (SI) to this paper.

Both species, anionic (M = Cr) and neutral (M = Mn), have very similar geometries, namely staggered conformations with dihedral angle $\angle C_{eq}-M-I_c-I_t$ of ~45°. Estimation of the rotational barrier around the $M-I_c$ axis showed that the eclipsed geometry is higher in energy by 2.4 and 3.8 kcal/mol for Cr- and Mn-derivatives, respectively. The full energy profiles for rotation are presented in Figure 6. Rotation around the $M-I_c$ bond thus encounters only a small barrier. This is consistent with weak nonbonding interactions between uncoordinated iodine atoms and carbonyl ligands.

"Side-on" coordination of an I_3^- by a metal center does not result in any notable changes in I_c-I_t bond lengths in
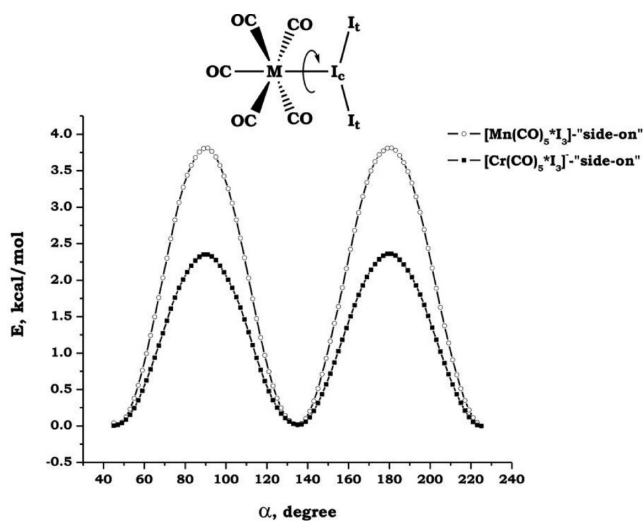
comparison with unperturbed I_3^-. There is only a slight bending of the coordinated triiodide, to an $\angle I-I-I$ of at most 166° (Table 1). The $M-I_c$ bond is slightly longer in the neutral manganese adduct (2.80 vs 2.73 Å for $[Cr(CO)_5 \cdot I_3]^-$ and $[Mn(CO)_5 \cdot I_3]$, respectively). Presumably, this is related to an increase of the Coulomb contribution to the bonding between $M(CO)_5^+$ and the I_3^-. Coordination of the triiodide by a metal center has, however, only minimal influence on the bonding of the metal with its CO ligands (Table 1).

"End-On" Adducts of I_3^-. Though the "side-on" bonded I_3^- complexes are important to us as the lead-in to our discussion of XeF_2 as a ligand (in a subsequent paper), they do not represent the most stable way that an I_3^- can bond to a metal fragment. The few known I_3^- complexes are, as we have seen, "end-on" bonded.[1,7,8] Indeed, our calculations find that the local minima for "end-on" bonded I_3^- complexes with $[Cr(CO)_5]$ and $[Mn(CO)_5]^+$ are lower in energy than the "side-on" minima by 7−13 kcal/mol (Figure 5b). Selected geometrical parameters are listed in Table 1.

As for "side-on" adducts, the equilibrium geometries of the "end-on" isomers correspond to staggered conformations, while the eclipsed conformations are transition states in rotation. A close look at geometrical parameters for "end-on" adducts (Table 1) reveals that $M-I_t$ bond in these compounds is slightly shorter than that in "side-on" analogues (2.78 vs 2.80 Å for M = Cr and 2.70 vs 2.73 Å for M = Mn, respectively). Though the difference is small, it correlates with the relative stability of the isomers.

In contrast to "side-on" adducts, where no significant changes (relative to free I_3^- species) in I_c-I_t bond lengths were found, "end-on" derivatives are significantly asymmetric in the I_3^- part. The bond between coordinated iodine atom I_t and I_c becomes notably longer, whereas $I_c-I'_t$ is much shortened in comparison with an unperturbed I_3-anion (Table 1). There are two perspectives on this: First, such an asymmetry is typical for I_3^- itself in an asymmetrical environment,[1] and cannot be very costly energetically. Second, while the $I_c-I'_t$ bond is still by ca. 0.15 Å longer than that in the neutral I_2, the tendency is clear: the formation of the "end-on" isomer could be viewed as the first step on the way to formation of a metal iodide, and elimination of diiodine molecule. We will return to this perspective.

Isomerization between "End-On" and "Side-On" Bound I_3^- Complexes. Given the existence of two isomers, it makes sense to inquire about their interconversion. Our

Figure 6. Energy as a function of angle of rotation around the $M-I_c$ bond for $[Cr(CO)_5 \cdot I_3]^-$ and $[Mn(CO)_5 \cdot I_3]$.

Table 2. Calculated Parameters of Electronic Structure of $[M(CO)_5\cdot I_3]^{n-}$-"Side-On", $[M(CO)_5\cdot I_3]^{n-}$-"End-On", $[M(CO)_5\cdot I]^{n-}$ (n = 1 for M = Cr and n = 0 for M = Mn), and $[M(CO)_5\cdot I_2]^{n+}$ (n = 0 for M = Cr and n = 1 for M = Mn), and for Their Parent Fragments, $[M(CO)_5]^{n+}$ and I_2, I_3^- with All Energetic Estimates in kcal/mol

	Cr				Mn					
	$[Cr(CO)_5\cdot I_3]^-$				$[Mn(CO)_5\cdot I_3]$					
param	"side-on"	"end-on"	$[Cr(CO)_5\cdot I]^-$	$[Cr(CO)_5\cdot I_2]$	"side-on"	"end-on"	$[Mn(CO)_5\cdot I]$	$[Mn(CO)_5\cdot I_2]^+$	I_3^-	I_2
$q(M)$	−1.46	−1.47	−1.47	−1.50	−0.77	−0.81	−0.82	−0.76		
$q(I_c)$	+0.22	−0.17	−0.45	+0.30	+0.23	−0.20	−0.29	+0.27	−0.07	0.00
$q(I_t)$	−0.41	−0.06		−0.04	−0.35	−0.04		+0.13	−0.46	0.00
$q(I'_t)$		−0.33				−0.11				
b.o. $(M–I^*)$	0.35	0.36	0.28	0.49	0.39	0.41	0.43	0.38		
b.o. $(I_c–I_t)$	0.51	0.38		0.85	0.50	0.17		0.98	0.53	1.03
b.o. $(I_c–I'_t)$		0.66				0.87				
$E^{(2)}$ $(M \rightarrow L)^*$	12	0	0	18	2	0	0	2		
$E^{(2)}$ $(L \rightarrow M)^*$	102	103	103	159	113	118	127	121		
$E(\text{bonding})^a$	−28	−35	−53	−20	−114	−127	−160	−28		
$E_a^{\ b}$	+10				+11					

^{a}Values of the bonding energy $E(\text{bonding})$ were calculated as the energy difference between the absolute energy of independently optimized adduct and parent fragments, $E(\text{bonding}) = E_{abs}([M(CO)_5\cdot I_3]^{n-}) - E_{abs}(M(CO)_5^{m+}) - E_{abs}(I_3^-)$, where [$n$ = 1; m = 0] for M = Mn and [n = 0; m = 1] for M = Cr. Such estimation includes the M–I_c bond strength as well as any other additional interactions, such as back-bonding, stabilizing the target configuration. A negative sign of the bonding energy thus defined corresponds to stable compounds, while a positive sign indicates that formation of such molecules is not favorable. $^b E_a$ designates the activation energy for the transition between "side-on" and "end-on" isomers of $[M(CO)_5\cdot I_3]^{n-}$ adducts.

calculations show activation energy (E_a) for transition from "side-on" to "end-on" isomer of *ca.* 10 kcal/mol for both metals (Table 2). Isomerization by decoordination of the entire ligand and recoordination at a second site would be more costly in energy. The transition states for the interconversion are shown in Figure 7. Such relatively low values mean that these isomers might coexist at room temperature, while decreasing the temperature could result in isolation of the more stable adduct.
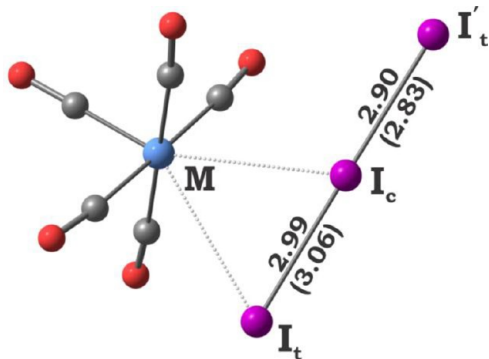

Figure 7. Transition state for the interconversion between "end-on" and "side-on" isomers of $[M(CO)_5\cdot I_3]^{n-}$ (n = 0 for M = Mn and n = 1 for M = Cr). Selected distances are given in Å for M = Cr (for M = Mn in parentheses).

Electron Density Shifts on Coordination. We begin an NBO analysis of the electronic structure of I_3^- adducts, by looking at the charges on the various atoms (Table 2). Note first the negative charge on the metal center in all complexes. The absolute value of this charge is larger for M = Cr than that for M = Mn, likely connected with initial positive charge of $[Mn(CO)_5]^+$ bonding partner. Formation of an adduct leads to an increase of negative charge on the central metal atom from −1.02 to *ca.* −1.50 in the case of Cr-derivatives, and from −0.40 to *ca.* −0.80 for Mn-containing compounds, due to partial electron transfer from the coordinated iodine ligand to

the metal. This is supported by positive charge of the I_c atom, while I_t atoms remain negative and undergo only slight change, most pronounced for M = Mn.

In the case of "end-on" adducts, the situation with respect to electron densities is very similar (Table 2). The charge of I_t, the iodine connected to the metal center, is substantially reduced (−0.17 and −0.20 for Cr- and Mn-derivatives) in comparison with the charge in the unperturbed I_3-anion (−0.46), as well as compared to the "side-on" adducts (−0.41 and −0.35 for M = Cr and Mn, respectively). Such a reduction of the negative charge of the iodine atoms on coordination by a metal center follows the trend observed for I_c in "side-on" isomers, where this is more pronounced (I_c was found to be even positive!).

For comparison, Table 2 also contains complexes with I^- and I_2. Note how similar the charges on the metal are in I^-, I_2, I_3^- complexes. Donation is the main feature here.

Detailed NBO Analysis of Bonding. In the framework of an NBO analysis, the strength of donor−acceptor interaction between selected fragments can be quantified by examining possible interactions between filled (donor) Lewis-type NBOs and empty (acceptor) non-Lewis NBOs, evaluating their energetic importance by using second-order perturbation theory in the NBO basis. Because these interactions lead to loss of occupancy from localized NBOs of an idealized Lewis structure to empty non-Lewis orbitals (and thus to departure from an idealized Lewis structure description), they are referred to as delocalization corrections to the zeroth-order natural Lewis structure.[6]

For each donor NBO (i) and acceptor NBO (j), the stabilization energy, $E^{(2)}$, associated with delocalization $i \rightarrow j^*$, is estimated as

$$\Delta E^{(2)}_{i \rightarrow j*} = -2 \cdot (\langle \sigma_i | \mathbf{F} | \sigma_j \rangle)^2 / (\varepsilon_{j*} - \varepsilon_i)$$

where $\mathbf{F}$ is an effective orbital Hamiltonian (Fock or Kohn–Sham operator) and $\varepsilon_i = \langle \sigma_i | \mathbf{F} | \sigma_i \rangle$ and $\varepsilon_{j*} = \langle \sigma_{j*} | \mathbf{F} | \sigma_{j*} \rangle$ are orbital energies for donor and acceptor NBOs, respectively. In interpreting such estimates, it should be noted that this

approach is only performed at the SCF level of theory (i.e., the Fock or Kohn−Sham operator is analyzed in the basis of the NBOs). Also, only bonding interactions are considered (i.e., antibonding contributions are not covered by NBO and must be calculated separately). So, as one can see in Table 2, for instance, for $[Cr(CO)_5 \cdot I_3]^-$ the L → M dominant second order perturbation term is 102 kcal/mol, but the net E(bonding) is only −28 kcal/mol [E(bonding) is defined so that it is negative for a molecule bound relative to the fragments]. The difference is due to other terms, mostly repulsive, in the energy expression. We nevertheless find the $E^{(2)}$ perturbation terms strongly indicative of the nature of the bonding in these molecules.

NBOs of I_3^-. The NBOs of a molecule are in principle the best single configuration orbitals for a molecule. As we discussed previously,[5] they resemble and yet may differ from the canonical orbitals of a molecule, which are more familiar to the community. In this section, we illustrate the NBOs of I_3^- (Figure 8) and compare them with the canonical MO picture shown earlier (Figure 4).
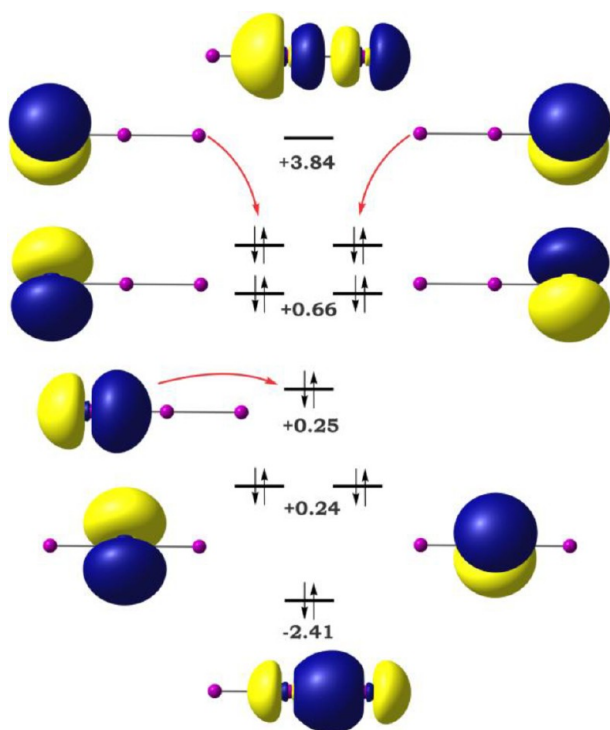

**Figure 8.** Natural bond orbitals for the I_3^- ion, along with their energies (in eV). The energy scale is schematic.

As we recently found in the case of neutral I_2 molecule, the formation of NBOs brings about a substantial localization of π-type doubly occupied molecular orbitals, a localization that makes chemical sense. The six such canonical π-orbitals of Figure 4 are now transformed into six p-type lone pairs localized on individual iodine atoms (two lone pairs per atom, Figure 8). The four lone pairs localized on I_t atoms are slightly higher in energy than the two of on the central iodine; this is consistent with the negative charge at the terminal atoms. And this might bring some preference for coordination of I_3^- by Lewis acids to terminal sites.

The situation in the σ-system is different and very interesting. The three canonical MOs σ_1, σ_2, and σ_3 are replaced in the

NBO scheme by three σ orbitals breaking left−right symmetry. The lowest is a σ-bond localized on I_2−I_3; it has a σ^* partner that is unfilled. The middle orbital is a lone pair, a p-orbital quite localized on I_1.

Of course, there is a second NBO solution with equal weight, in which the localization is switched to a lone pair of I_3, and I_1−I_2 σ and σ^* levels. The NBO picture recovers the two main contributors to the VB picture of I_3^-,[13] shown in Scheme 1.

Scheme 1
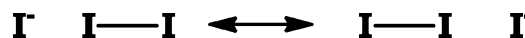
What changes does an NBO perspective bring to us for the $M(CO)_5$ fragment? The d-type levels remain pretty localized but change in interesting small ways. Figure 9 compares the canonical LUMO (which will figure prominently in the bonding) with the NBO LUMOs of $[Cr(CO)_5]$ and $[Mn(CO)_5]^+$.

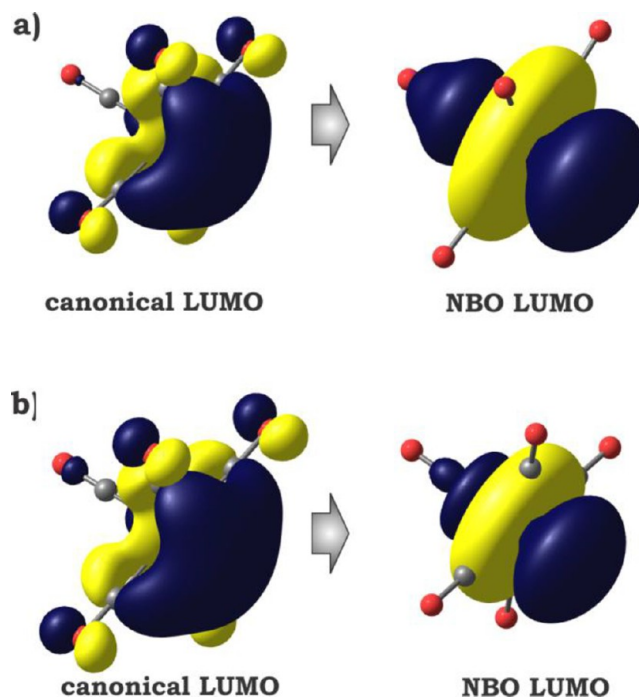**Figure 9.** Comparison of canonical LUMOs with corresponding NBO LUMOs of (a) $[Cr(CO)_5]$ and (b) $[Mn(CO)_5]^+$.

Notice first the more "directed" hybrid nature of the canonical MO, the result of more mixing of M p_z (z is chosen along the 4-fold axis). That hybridization generates π-bonding capability in the a_1, note the CO π^* mixing. In the unfilled Lewis acceptor orbitals (LAOs) of $M(CO)_5$ there is little p_z character, and little CO admixture. The LAO orbital is mainly metal $3d_{z^2}$, with a little 4s character. Notice also the expected "shrinkage" of the MO in the cationic $[Mn(CO)_5]^+$ compared to the neutral $[Cr(CO)_5]$.

With the difference between canonical MOs and NBOs in mind, we now can show the outcome of the NBO analysis.

Nature of I_3^- Bonding. The aforementioned ligand-to-metal (L → M, Table 2) contribution to the total donor−acceptor interaction dominates over the metal-to-ligand one (M → L, here L designates the I_3^--ligand) and constitutes the major part of the total bonding. Figure 10 shows the single
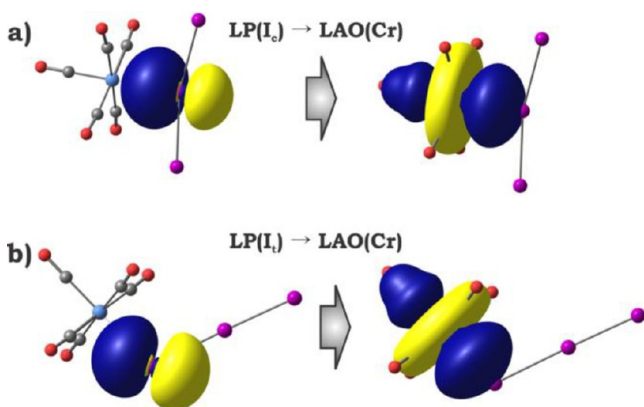
Figure 10. Major contributor to the L → M interaction in an NBO analysis for (a) "side-on" and (b) "end-on" adducts of I_3^- with $[Cr(CO)_5]$ (for analogous orbital pictures in the case of $[Mn(CO)_5]^+$, see SI). LP and LAO designate lone pair and Lewis acceptor orbital, respectively.

dominant interaction for both "end-on" and "side-on" bonded complexes for the $[Cr(CO)_5]$; the orbitals are similar for the $[Mn(CO)_5]^+$ bonding. The M → L term was found to be almost negligibly small for all compounds under consideration; triiodide is not acting as an acceptor, nor would it have been expected to do so.

We see clear donation from a localized iodine-based lone pair (at I_t for the "end-on" complex, at I_c for the "side-on" bonded one) to the LAO of $M(CO)_5$.

In an NBO analysis it is also possible to estimate quantitatively the electron transfer from a donor NBO to an acceptor one, considering that before interaction these orbitals are doubly occupied and completely empty, respectively. Such estimations show that electron density transfer to the $M(CO)_5$ acceptor orbital is very similar for all adducts, ca. 0.3–0.4e. The difference between "end-on" and "side-on" isomers is small.

Completing the picture of the electronic structure of "side-on" and "end-on" adducts, it is worthwhile to take a quick look at what changes happen in I_3^- upon coordination by $M(CO)_5$. In contrast to "side-on" bonding, significant perturbations in geometrical parameters of iodine fragment were observed for "end-on" complexes (see Table 1). In the latter, the I–I bond involved in bonding with metal center becomes longer, while the other I–I bond is shortened.

One might expect that these changes reflect a difference in the internal 4e–3c bonding between iodine atoms in I_3^-. In isolated I_3^-, which can be considered as the outcome of donor–

acceptor interaction between I^- and I_2, one can inquire of the strength of this interaction in the framework of NBO perturbation theory. One obtains a large interaction of 133 kcal/mol.[14] In "side-on" adducts the same interaction (in the I_3^- moiety) amounts to 125 and 134 kcal/mol for Cr- and Mn-derivatives, respectively. In contrast, a dramatic decrease of the strength of $I^-\cdots I_2$ interaction was found in the "end-on" isomers. Estimated values are 51 and 20 kcal/mol for M = Cr and Mn, respectively. This striking decrease in $I^-\cdots I_2$ interaction supports the above-mentioned suspicion that the "end-on" adducts could be considered as the first step in decomposition of a coordinated I_3-anion to a metal iodide and a neutral I_2 molecule. We will return to this subject.

EDA Analysis of Bonding. The NBO analysis points to a significant influence of charge on the total bonding energy. In order to clarify the interplay between electrostatic and covalent contributions to the total bonding energy, as well as to shed more light on the electronic structure of these compounds, an EDA analysis was performed (Table 3).

First of all, one can observe that values of ΔE_{int} are very similar to values of $-D_e$, indicating very small preparation energies (ΔE_{prep}). The calculated ΔE_{int} is clearly influenced by the charges of the interacting fragments; the neutral adduct, the product of interaction of a cation and an anion, is much more strongly bound. The mode of coordination matters too. We already pointed to another sign of this: the shorter Mn–I distances shown in Table 1. But the bonding differential is surprising.

In the EDA one can decompose the total interaction energy (ΔE_{int}) into attractive (ΔE_{orb} and ΔE_{elstat}) and repulsive (ΔE_{Pauli}) terms. Let us first consider the influence of metal fragment on M–I bonding. That there would be a pronounced electrostatic component for $[Mn(CO)_5]^+$ was expected (Table 3). The orbital contribution (often assigned to the covalent or donor–acceptor part of bonding) is by ca. 30 kcal/mol higher in the case of cationic Mn compounds interacting with I_3^- than those in Cr derivatives. The absolute value of the repulsive ΔE_{Pauli} also increases in the same direction. The coordination mode ("side-on" vs "end-on") was found to have no influence on the trend in any of the attractive or repulsive terms.[15]

I^- and I_2 Complexes. The obvious question that must be faced in thinking about complexation of I_3^- is the potential coordination-induced fragmentation of the ligand to I^- and I_2, and possible bonding of one of these new ligands to the metal fragment. The calculated asymmetry in the "end-on" I_3^- complexes (Table 1) suggests that the product of a fragmentation would be the iodide. For the sake of comparison,

Table 3. Results of an EDA Analysis for $[M(CO)_5\cdot I_3]^{n-}$-"Side-On", $[M(CO)_5\cdot I_3]^{n-}$-"End-On", $[M(CO)_5\cdot I]^{n-}$ ($n = 1$ for M = Cr and $n = 0$ for M = Mn), and $[M(CO)_5\cdot I_2]^{n+}$ ($n = 0$ for M = Cr and $n = 1$ for M = Mn) (PBE0/TZ2P/ZORA)

	Cr				Mn			
	$[Cr(CO)_5\cdot I_3]^-$				$[Mn(CO)_5\cdot I_3]$			
param	"side-on"	"end-on"	$[Cr(CO)_5\cdot I]^-$	$[Cr(CO)_5\cdot I_2]$	"side-on"	"end-on"	$[Mn(CO)_5\cdot I]$	$[Mn(CO)_5\cdot I_2]^+$
ΔE_{int}	−29	−35	−51	−21	−118	−135	−160	−30
ΔE_{orb}	−31	−35	−45	−37	−59	−74	−82	−45
ΔE_{elstat}	−39	−48	−69	−32	−116	−133	−171	−27
ΔE_{Pauli}	+41	+48	+63	+48	+56	+72	+93	+43
$-D_e{}^a$	−27	−34	−49	−19	−115	−127	−155	−29
ΔE_{prep}	+3	+1	+2	+2	+3	+9	+5	+2

$^a(-D_e) = E(\text{molecule}) - E(\text{fragments})$; negative for bound molecules. Only interactions between the metal pentacarbonyl fragment and iodine-containing ligands (I^-, I_2, and I_3^-) were considered.

adducts with I^- and neutral I_2 molecule were calculated at the same level of theory (Figure 11 and Table 4). By using the
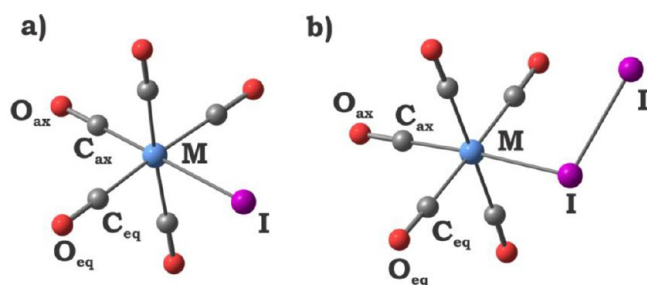

Figure 11. Equilibrium geometry for $[M(CO)_5 \cdot I]^{n-}$ ($n = 1$ for M = Cr and $n = 0$ for M = Mn) and $[M(CO)_5 \cdot I_2]^{n+}$ ($n = 1$ for M = Mn and $n = 0$ for M = Cr) along with labeling scheme.

latter (I_2), we can trace the importance of the electrostatic component of the bonding between an iodine-based fragment and neutral or positively charged organometallic complex.

Complexes of I^- are reasonably well-represented in the experimental literature.[16] To our knowledge, there are only two I_2 complexes of this type[17] (where I_2 molecule is a donor). In contrast, there are several complexes (still not too many) with I_2 as an acceptor (one of these was depicted in Figure 2). The nature of the bonding in both types (all with late transition metals) was theoretically investigated in detail by us recently.[5] In this part, we consider I^- and I_2 adducts with early transition metal complexes (Cr- and Mn-based).

Comparison of equilibrium configurations of $[M(CO)_5 \cdot I]^{n-}$ with that of $[M(CO)_5 \cdot I_3]^{n-}$ (both "side-on" and "end-on"; $n = 1$ for M = Cr and $n = 0$ for M = Mn) showed few differences. The M−I bond length becomes slightly shorter in the monoiodides, possibly due to decrease of steric interaction with carbonyls, or to I^- being a stronger ligand.

A contrasting situation occurs in the case of neutral I_2 molecules as an adduct (Figure 11 and Table 4). While for the Mn-derivative no significant changes were observed in M−I separation (2.73, 2.69, and 2.71 Å for $[Mn(CO)_5 \cdot I_3]$-"side-on", $[Mn(CO)_5 \cdot I]$, and $[Mn(CO)_5 \cdot I_2]^+$, respectively), the Cr−I bond length was found to be much shorter in the I_2 complex than that in the I_3-adduct (2.65 Å in $[Cr(CO)_5 \cdot I_2]$ vs 2.80 Å in both $[Cr(CO)_5 \cdot I]^-$ and $[Cr(CO)_5 \cdot I_3]^-$-"side-on").

What might be the reason for such Cr−I bond shortening and what is its relationship to the bonding energy (as a measure of thermodynamic stability) in the target adducts? Surprisingly, even though the Cr−I distance is short, $[Cr(CO)_5 \cdot I_2]$ has the lowest magnitude of a bonding energy in the group, −20 kcal/

mol, while for the complex $[Cr(CO)_5 \cdot I]^-$ E(bonding) = −53 kcal/mol, which is substantially larger in magnitude than for any of Cr-based adducts of I_3^- (−28 kcal/mol and −35 kcal/mol for "side-on" and "end-on" isomers, respectively). One factor that might influence the Cr−I bond length in $[Cr(CO)_5 \cdot I_2]$ and make it shorter then in adducts with anionic I^- and I_3^- is the substantially smaller radius of the interacting atom for neutral I_2. The electron density of I^- and I_3^- is very diffuse, and consequently, these ligands are likely to interact with the metal center at longer distance. We are grateful to a reviewer for this suggestion.

For the Mn-derivatives, reducing the important electrostatic component of bonding results in a dramatic fall in the magnitude of the Mn−I bonding energy in $[Mn(CO)_5 \cdot I_2]^+$ (−28 kcal/mol), in comparison with that in any other adduct considered here (−160, −114, and −127 kcal/mol for $[Mn(CO)_5 \cdot I]$, $[Mn(CO)_5 \cdot I_3]$-"side-on", and $[Mn(CO)_5 \cdot I_3]$-"end-on", respectively). Electrostatic interactions clearly dominate the overall bonding of L_nM to I^-, I_2, and I_3^- (Table 2).

Nature of M−I Interaction in I^- and I_2 Adducts. As in adducts of the I_3-anion with the same metal fragments, an NBO analysis of complexes of I^- and I_2 (Table 2) revealed that the aforementioned L → M component of donor−acceptor bonding dominates over the M → L one. At the same time, the absolute value of the interaction energy fluctuates within a subseries. For example, for Cr compounds, the L → M contribution was found to be almost equal for adducts with I_3^- and I^-, whereas it rose significantly (by *ca.* 50 kcal/mol) for the neutral I_2. There is no such jump in energy for Mn compounds. The nature of the orbitals involved in L → M interaction is illustrated in Figure 12 for M = Cr (for Mn-derivatives see SI).

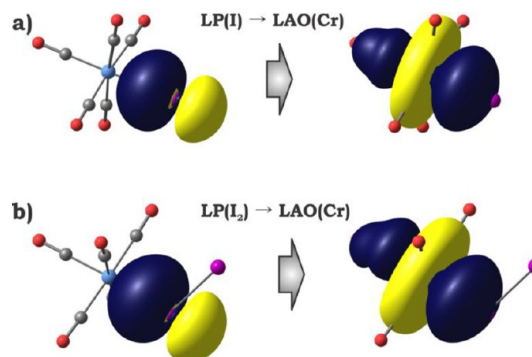**Figure 12.** Major contributor to the L → M interaction in an NBO analysis for adducts of I^- (a) and I_2 (b) with $[Cr(CO)_5]$ (the analogous orbital representation in the case of $[Mn(CO)_5]^+$ can be found in SI).

Table 4. Selected Computed Geometrical Parameters for $[M(CO)_5 \cdot I_2]^{n+}$ ($n = 0$ for M = Cr and $n = 1$ for M = Mn) and $[M(CO)_5 \cdot I]^{n-}$ and for I_2 (RIJCOSX-PBE0/TZVP/ZORA; Bond Lengths in Å, Angles in Degrees)

	Cr		Mn		
param	$[Cr(CO)_5 \cdot I]^-$	$[Cr(CO)_5 \cdot I_2]$	$[Mn(CO)_5 \cdot I]$	$[Mn(CO)_5 \cdot I_2]^+$	I_2
M−I	2.80	2.65	2.69	2.71	
I−I		2.75		2.70	2.69
M−C_{eq}	1.88	1.90	1.86	1.88	
M−C_{ax}	1.82	1.85	1.80	1.83	
(C−O)$_{eq}$	1.15	1.14	1.13	1.13	
(C−O)$_{ax}$	1.16	1.14	1.14	1.13	
∠M−I−I		110.7		106.2	
∠I−I−M−C_{eq}		46.7		42.5	
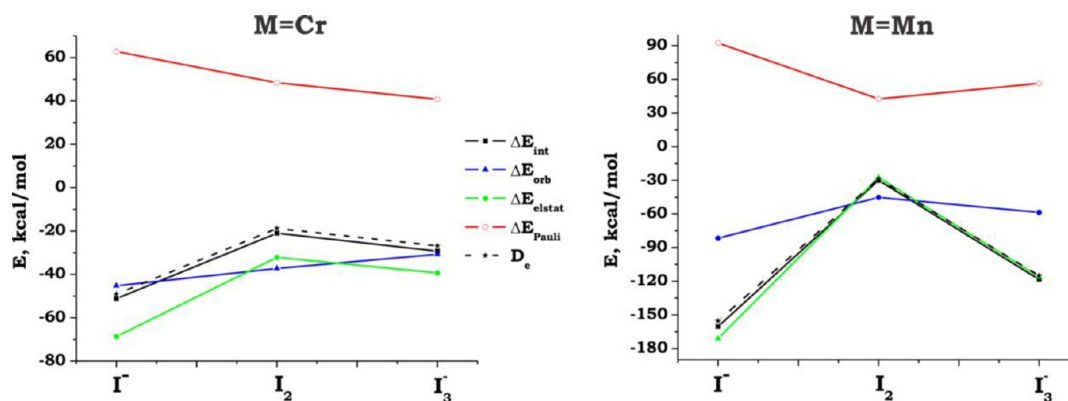
Figure 13. EDA analysis for $[M(CO)_5 \cdot I_3]^{n-}$-"side-on", $[M(CO)_5 \cdot I]^{n-}$ ($n = 1$ for M = Cr and $n = 0$ for M = Mn), and $[M(CO)_5 \cdot I_2]^{n+}$ ($n = 0$ for M = Cr, left, and $n = 1$ for M = Mn, right) (PBE0/TZ2P/ZORA).

The neutral I_2 molecule in the target complexes shows essentially the same type of reactivity (acting as a donor through a localized I lone pair) as we found in the I_2 adduct with a Rh(II) paddle-wheel metal fragment.[5]

These trends in the L → M term correlate well with NBO-derived M−I bond orders. In the case of Cr compounds, the highest bond order was observed for the neutral I_2-adduct (0.49), while for anionic species the M−I bond order was substantially smaller (0.35 and 0.28 for $[Cr(CO)_5 \cdot I_3]^-$ and $[Cr(CO)_5 \cdot I]^-$, respectively). In contrast, changes in the nature of iodine ligand in Mn adducts did not influence notably the Mn−I bond order. This might indicate a larger contribution from an electrostatic bonding term.

Interestingly, the above-mentioned trend in total bonding energy does not coincide with trends in the L → M part of bonding as evaluated by NBO perturbation theory (Table 2). One may guess that the main reason for this disagreement lies, perhaps, in the strong influence of electrostatics, different for different iodine fragments. This supposition is beautifully confirmed by the EDA analysis (Figure 13 and Table 3). As expected, the electrostatic term is much more pronounced in the case of interaction between two charged fragments $[Mn(CO)_5]^+$ and I_3^- or I^-, whereas the smallest contribution from ΔE_{elstat} was found in the case of neutral $[Cr(CO)_5 \cdot I_2]$.

Fragmentation of a Complexed Triiodide. With the bonding of an iodide ligand analyzed, we can return to the energetics of the potential fragmentation process to a metal iodide and free diatomic iodine for our model adducts, complexed triiodides. First of all, for both metal fragments this reaction is an uphill process. The energy of the bonding between $[M(CO)_5 \cdot I]^{n-}$ ($n = 1$ for M = Cr and $n = 0$ for M = Mn) and a single I_2 molecule is −20 and −6 kcal/mol, for Cr- and Mn-derivatives, respectively. This finding is opposite to the trend in the M−I bonding energy in $[M(CO)_5 \cdot I]^{n-}$ (Table 2) and fully supports the conclusion about the importance of the electrostatic term. The stronger the M−I bond is (with a maximal electrostatic contribution to the interaction), the weaker the bonding is between I^- and I_2. The trend also agrees with what NBO perturbation theory gives for the "end-on" adducts of both metal fragments. The analogous bonding energy for I^- (i.e., the bonding energy of I^- with I_2 to give I_3^-) is equal to −38 kcal/mol. It is clear that a complexed triiodide will resist loss of I_2, even if the coordination to the metal makes the geometry of the I_3^- asymmetrical.

CONCLUSIONS

We find stabilizing interactions of I_3^- with $[Cr(CO)_5]$ and $[Mn(CO)_5]^+$ for both "end-on" and "side-on" (through central I of I_3^-) coordination, with the "end-on" bonded isomer being slightly more stable. Asymmetries in the I−I distances of the "end-on" adduct lead us to consider as well the energetics of I^- and I_2 bonded to the same metal fragments. Detailed analysis of the M−I bonding in the various compounds revealed that electrostatic interactions dominate over the covalent term, except for adducts with neutral I_2 as a ligand. For the latter, the bonding energy was found to be the smallest.

Summarizing the theoretical results obtained for adducts of iodine ligands (I^-, I_2, I_3^-) with model organometallic fragments, $[M(CO)_5]^{n+}$ ($n = 0$ for M = Cr and $n = 1$ for M = Mn), one finds that the strongest M−I bond is formed for adducts with the simple iodide. This is the driving factor for the potential decomposition of "end-on" adducts of I_3^- to metal iodides and a free neutral I_2 molecule. However, this reaction was found to be uphill.

Complete dissociation would lose donor−acceptor interactions between coordinated I^- (donor) and I_2 (acceptor). These are substantial, so under certain circumstances the "end-on" bonded I_3^- complex is stabilized. This perspective is supported experimentally, by the known structures of a number of "end-on" complexes.[1,7,8] The stability of "side-on" adducts, less prone to lose I_2, is calculated to be lower than that of "end-on" analogues. The reaction barrier to "side-on" to "end-on" interconversion is calculated as +10 and +11 kcal/mol for Cr- and Mn-derivatives, respectively. So, there may be a chance to obtain the "side-on" bonded isomers, but only at low temperature.

APPENDIX

Computational Details

Geometry optimizations of all systems under consideration were performed at two levels of theory. The first approach makes use of full electron relativistically recontracted basis sets of triple-zeta quality augmented by one (TZVP) or by two (TZVPP) polarization functions. These basis sets were used in a segmented all-electron relativistically contracted form (the so-called SARC basis sets). The effectiveness of basis sets of this type was previously tested.[18] The key feature of such an approach is complete consideration of all electrons of the model and direct accounting of relativistic corrections. Additionally, there are no problems with interaction between

core and valence electrons, difficulties that sometimes appear when doing calculations using effective core potentials (ECP).

Within this first approach, we made use of density functional theory (DFT), employing the hybrid correlation-exchange parameter-free functional of Perdew−Burke−Ernzerhof (PBE0).[19] To accelerate calculations, the resolution-of-identity (RI) algorithm was applied using the chain-of-sphere approach,[20] specifically developed recently for hybrid functionals (RIJCOSX in the ORCA[21] software terminology). This technique was found to be very efficient, with negligible loss in accuracy by comparison with standard hybrid functionals. Scalar relativistic effects have been incorporated by applying the zero-order regular approximation (ZORA). All these calculations were carried out by using the ORCA program suite (version 2.8.0, second update).[4]

The second approach used the standard PBE0 functional without additional approximations. All atoms were described by def2-TZVPP basis sets. Heavy elements such as iodine were described with the aid of relativistic effective core potentials with a small core (ecp-28-mwb). This set of calculations was performed using the Firefly[22] (version 7.1.G) program package.

In all cases, no symmetry restrictions were applied. All calculated structures correspond to local minima (no imaginary frequencies) on the corresponding potential energy surfaces, as determined by calculation of the full Hessian matrix, followed by estimation of frequencies in the harmonic approximation. The nature of any transition state (TS), aside from possessing a single imaginary frequency, was probed through the IRC (intrinsic reaction coordinate) technique, guaranteeing that the TS led to the target products or reactants. IRC calculations were performed using the Firefly program, at the level of theory mentioned above.

In the next step, optimized geometries were used to get insight into the electronic structure of our target systems in terms of natural bond orbitals (NBO).[23] Bond orders quoted are those from the Wiberg formulation[24] (so-called Wiberg bond indexes) incorporated in the NBO analysis. All computations were performed with GENNBO (version 5.0) program,[25] using the converged wavefunctions generated by Firefly and/or ORCA programs.

The bonding between metal pentacarbonyl and iodine-based fragments was further investigated by the energy decomposition analysis (EDA) developed by Morokuma[26] and by Ziegler and Rauk.[27] For this purpose, single-point calculations were performed by the ADF program package[28] with the same functional. All atoms were described by uncontracted Slater-type orbitals (STOs) with TZ2P quality as basis functions.[29] An auxiliary set of s, p, d, and f STOs was used to fit the molecular densities and to represent the Coulomb and exchange potentials accurately in each SCF cycle.[30] Scalar relativistic effects have been taken into account by ZORA.

The EDA bonding analysis focuses on the interaction energy ΔE_{int} on forming a bond A−B between two fragments A and B, in the frozen geometry of AB. This interaction energy may be divided into three main components (eq 1).

$$\Delta E_{int} = \Delta E_{elstat} + \Delta E_{Pauli} + \Delta E_{orb} \qquad (1)$$

The term ΔE_{elstat} corresponds to the classical electrostatic interaction between the unperturbed charge distributions of the prepared atoms or molecular fragments, and is usually attractive. The Pauli repulsion, ΔE_{Pauli}, is the energy change associated with the transformation from a simple product function of the fragments to the wavefunction $\psi^0 = N\hat{A}[\psi_A\psi_B]$,

which properly obeys the Pauli principle through explicit antisymmetrization (by the $\hat{A}$ operator) and renormalization of the product wavefunction.[31] This term, usually large and positive, contains the destabilizing interactions between electrons of the same spin on either fragment. This is where the four-electron two-orbital contributions of a one-electron model are to be found. The orbital interaction ΔE_{orb} accounts for charge-transfer and polarization effects.[32] One can get further insight; for example, the ΔE_{orb} term can be decomposed into contributions from each irreducible representation of the point group of the interacting system. To obtain the bond dissociation energy (BDE), D_e, the preparation energy ΔE_{prep}, which measures the relaxation of the fragments into their electronic and geometrical ground states, must be added to ΔE_{int} (eq 2).

$$\Delta E(-D_e) = \Delta E_{int} + \Delta E_{prep} \qquad (2)$$

For dissociation energies, we calculated each fragment in its optimized geometry and derived ΔE by eq 2. Further details on the EDA as well as a discussion of the above-mentioned terms can be found in the literature.[33]

■ ASSOCIATED CONTENT

ⓈSupporting Information

Additional tables, figures, and details. This material is available free of charge via the Internet at http://pubs.acs.org.

■ AUTHOR INFORMATION

Corresponding Author
*E-mail: rh34@cornell.edu.

Notes
The authors declare no competing financial interest.

■ ACKNOWLEDGMENTS

■ REFERENCES

(1) Svensson, P. H.; Kloo, L. *Chem. Rev.* **2003**, *103*, 1649.
(2) (a) Pimentel, G. C. *J. Chem. Phys.* **1951**, *19*, 446. (b) Hach, R. J.; Rundle, R. E. *J. Am. Chem. Soc.* **1951**, *73*, 4321.
(3) Bent, H. A. *Chem. Rev.* **1968**, *68*, 587.
(4) Bürgi, H. B.; Dunitz, J. D.; Shefter, E. *J. Am. Chem. Soc.* **1973**, *95*, 5065.
(5) Rogachev, A.Yu.; Hoffmann, R. *J. Am. Chem. Soc.* **2013**, *135*, 3262.
(6) Cambridge Crystallographic Data Center, http://www.ccdc.cam.ac.uk/.
(7) Blanchard, S.; Neese, F.; Bothe, E.; Bill, E.; Weyhermuller, T.; Wieghardt, K. *Inorg. Chem.* **2005**, *44*, 3636.
(8) (a) Gossage, R. A.; Ryabov, A. D.; Spek, A. L.; Stufkens, D. J.; van Beek, J. A. M.; van Eldik, R.; van Koten, G. *J. Am. Chem. Soc.* **1999**, *121*, 2488. (b) van Beek, J. A. M.; van Koten, G.; Dekker, G. P. C. M.; Wissing, E. *J. Organomet. Chem.* **1990**, *394*, 659. (c) van Beek, J. A. M.; van Koten, G.; Smeets, W. J. J.; Spek, A. L. *J. Am. Chem. Soc.* **1986**, *108*, 5010. (d) van Koten, G. *Pure Appl. Chem.* **1990**, *62*, 1155.
(9) Elian, M.; Hoffmann, R. *Inorg. Chem.* **1975**, *14*, 1058.
(10) (a) Ibrahim Al-Rafia, S. M.; Malcolm, A. C.; Liew, S. K.; Ferguson, M. J.; Rivard, E. *J. Am. Chem. Soc.* **2011**, *133*, 777. (b) Dostálová, R.; Dostál, L.; Růžička, A.; Jambor, R. *Organometallics* **2011**, *30*, 2405. (c) Ibrahim Al-Rafia, S. M.; Malcolm, A. C.;

7170

dx.doi.org/10.1021/ic400772u | *Inorg. Chem.* 2013, 52, 7161−7171

McDonals, R.; Ferguson, M. J.; Rivard, E. *Angew. Chem., Int. Ed.* **2011**, *50*, 8354. (d) Spinney, H. A.; Piro, N. A.; Cummins, C. C. *J. Am. Chem. Soc.* **2009**, *131*, 16233. (e) Cossairt, B. M.; Piro, N. A.; Cummins, C. C. *Chem. Rev.* **2010**, *110*, 4164. (f) Piro, N. A.; Cummins, C. C. *J. Am. Chem. Soc.* **2008**, *130*, 9524. (g) Piro, N. A.; Cummins, C. C. *Angew. Chem., Int. Ed.* **2009**, *48*, 934. (h) Piro, N. A.; Cummins, C. C. *Inorg. Chem.* **2007**, *46*, 7387.

(11) (a) Landrum, G. A.; Goldberg, N.; Hoffmann, R. *J. Chem. Soc., Dalton Trans.* **1997**, 3605. (b) Landrum, G. A.; Goldberg, N.; Hoffmann, R.; Minyaev, R. M. *New J. Chem.* **1998**, 883.

(12) Wolters, L. P.; Bickelhaupt, F. M. *ChemistryOpen* **2012**, *1*, 96.

(13) (a) Shaik, S. S.; Hiberty, P. C.; Oganessian, G.; Lefour, J.-M. *Nouv. J. Chim.* **1985**, *9*, 385. (b) Shaik, S. *New J. Chem.* **2007**, *31*, 2015.

(14) The seeming discrepancy between this large bonding term and the smaller *E*(bonding) has been discussed above.

(15) The small differences between the EDA dissociation energy of Table 3 and the *E*(bonding) of Table 2 are due to the differing level of the theory used.

(16) Adducts of neutral $Cr(CO)_5$: (a) Hong, J.; Tang, L.-F.; Yang, Z.; Zhai, Y.-P. *Transition Met. Chem.* **2005**, *30*, 439. (b) Brunner, H.; Leis, F.; Wachter, J.; Zabel, M. *J. Organomet. Chem.* **2001**, *628*, 39. (c) van Rooyen, P. H.; Geer, L.; Lotz, S. *Acta Crystallogr., Sect. C* **1990**, *C46*, 1432. (d) Bond, A. M.; Colton, R. *Inorg. Chem.* **1976**, *15*, 446. (e) Calhoun, H. P.; Trotter, J. *J. Chem. Soc., Dalton Trans.* **1974**, 377. Adducts of cationic $Mn(CO)_5^+$: (f) Reimer, K. J.; Shaver, A.; Quick, M. H.; Angelici, R. J. Pentacarbonylmanganese Halides. In *Inorganic Syntheses: Reagent for Transition Metal Complex and Organometallic Syntheses*; Angelici, R. J., Ed.; John Wiley & Sons, Inc.: Hoboken, NJ, 2007; Vol. *28*. (g) Blake, A. J.; Johnson, B. F. G.; Sieker, A. *Acta Crystallogr., Sect. C* **1992**, *C48*, 1708. (h) Hu, Y. F.; Bancroft, G. M.; Tan, K. H. *Inorg. Chem.* **2000**, *39*, 1255. (i) Schmidt, S. P.; Trogler, W. C.; Basolo, F. *J. Am. Chem. Soc.* **1984**, *106*, 1308.

(17) (a) Cotton, F. A.; Dikarev, E. V.; Petrukhina, M. A. *Angew. Chem., Int. Ed.* **2000**, *39*, 2362. (b) Cameron, T. S.; Passmore, J.; Wang, X. *Angew. Chem., Int. Ed.* **2004**, *43*, 1995.

(18) (a) Pantazis, D. A.; Chen, X.-Y.; Landis, C. R.; Neese, F. *J. Chem. Theory Comput.* **2008**, *4*, 908. (b) Buhl, M.; Reimann, C.; Pantazis, D. A.; Bredow, T.; Neese, F. *J. Chem. Theory Comput.* **2008**, *4*, 1449. (c) DeBeer George, S.; Neese, F. *Inorg. Chem.* **2010**, *49*, 1849.

(19) (a) Perdew, J. P.; Burke, K.; Ernzerhof, M. *Phys. Rev. Lett.* **1997**, *78*, 1396. (b) Perdew, J. P.; Burke, K.; Ernzerhof, M. *Phys. Rev. Lett.* **1996**, *77*, 3865.

(20) Neese, F.; Wennmohs, F.; Hansen, A.; Becker, U. *Chem. Phys.* **2009**, *356*, 98.

(21) Neese, F. *ORCA*; University of Bonn: Bonn, Germany, 2009.

(22) Granovsky, A. A. *Firefly, v.7.1.G*, http://classic.chem.msu.su/gran/gamess/index.html.

(23) (a) Weinhold, F.; Landis, C. A. *Valency and Bonding: A Natural Bond Orbital Donor−Acceptor Perspective*; Cambridge University Press: Cambridge, 2005. (b) Reed, A. E.; Curtiss, L. A.; Weinhold, F. *Chem. Rev.* **1988**, *88*, 899−926.

(24) Wiberg, K. B. *Tetrahedron* **1968**, *24*, 1083−1096.

(25) Glendening, E. D.; Badenhoop, J. K.; Reed, A. E.; Carpenter, J. E.; Bohmann, J. A.; Morales, C. M.; Weinhold, F. *NBO 5.0*; University of Wisconsin: MadisonWI, 2001.

(26) Morokuma, K. *J. Chem. Phys.* **1971**, *55*, 1236−1244.

(27) (a) Ziegler, T.; Rauk, A. *Inorg. Chem.* **1979**, *18*, 1558−1565. (b) Ziegler, T.; Rauk, A. *Inorg. Chem.* **1979**, *18*, 1755−1759.

(28) (a) Fonseca Guerra, C.; Snijders, J. G.; te Velde, G.; Baerends, E. J. *Theor. Chem. Acc.* **1998**, *99*, 391−403. (b) *ADF2008.01*; SCM, Vrije Universiteit: Amsterdam, Netherlands, http://www.scm.com. (c) te Velde, G.; Bickelhaupt, F. M.; Baerends, E. J.; Fonseca Guerra, C.; van Gisbergen, S. J. A.; Snijders, J. G.; Ziegler, T. *J. Comput. Chem.* **2001**, *22*, 931−967.

(29) Snijders, J. G.; Baerends, E. J.; Vernooijs, P. *At. Data Nucl. Data Tables* **1982**, *26*, 483.

(30) Krijn, J.; Baerends, E. J. *Fit Functions in the HFS-Method, Internal Report (In Dutch)*; Vrije Universiteit: Amsterdam, Netherlands, 1984.

(31) Bickelhaupt, F. M.; Baerends, E. J. In *Review in Computational Chemistry*; Wiley-VCH: New York, 2000; Vol. *15*.

(32) Bickelhaupt, F. M.; Nibbering, N. M. M.; van Wezenbeek, E. M.; Baerends, E. J. *J. Phys. Chem.* **1992**, *96*, 4864−4873.

(33) (a) Lein, M.; Frenking, G. In *Theory and Application of Computational Chemistry*; Dekstra, C., Ed.; Elsevier: New York, 2005. (b) von Hopffgarten, M.; Frenking, G. In *Computational Inorganic and Bioinorganic Chemistry*; Solomon, E., Ed.; Wiley: New York, 2009; pp 3−15. (c) Lein, M.; Szabo, A.; Kovac, A.; Frenking, G. *Faraday Discuss.* **2003**, *124*, 365. (d) Frenking, G.; Wichmann, K.; Frohlich, N.; Loschen, C.; Lein, M.; Frunzke, J.; Rayon, V. M. *Coord. Chem. Rev.* **2003**, *238−239*, 55−82. (e) Krapp, A.; Bickelhaupt, F. M.; Frenking, G. *Chem.—Eur. J.* **2006**, *12*, 9196−9216. (f) Krapp, A.; Frenking, G. *J. Comput. Chem.* **2007**, *28*, 15−24. (g) von Hopffgarten, M.; Frenking, G. *Wiley Interdisc. Rev.: Comput. Mol. Sci.* **2012**, *2*, 9196.